Simplifying the electronic wedge brake system model through model order reduction techniques

Mohd Hanif Che Hasan[1], Mohd Khair Hassan[2], Fauzi Ahmad[3], Mohammad Hamiruce Marhaban[2], Sharil Izwan Haris[4], Ehsan Arasteh[5]

[1]Department of Electrical Engineering Technology, Faculty of Electrical Technology and Engineering, Universiti Teknikal Malaysia Melaka, Melaka, Malaysia
[2]Department of Electrical and Electronic Engineering, Faculty of Engineering, Universiti Putra Malaysia, Serdang, Malaysia
[3]Department of Automotive, Faculty of Mechanical Technology and Engineering, Universiti Teknikal Malaysia Melaka, Melaka, Malaysia
[4]Kolej Kemahiran Tinggi MARA Masjid Tanah, Melaka, Malaysia
[5]Department of Mechanical and Aerospace Engineering, University of California, California, United States

Article Info

ABSTRACT

The electronic wedge brake (EWB) uses self-reinforcement principles to optimise stopping power, but its mathematical model has various actuation angles and system dynamics making controller design complex and computationally burdensome. Therefore, the model order reduction (MOR) is made based on three factors that may have a negligible influence on the EWB system: the motor inductance, lead screw axial damping, and wedge mass. Six reduced order model (ROM) types were proposed when one, two, or all factors were ignored. The ROM accuracy was analysed using the frequency and time domain. The percentage of root means square error (RMSE) response value between the EWB benchmark model, and the predicted response based on the ROM was found to be less than 2%, with ROM size reduced from 5 to 2 orders. It guarantees that the new ROM series will be useful for simpler EWB controller design. The proposed ROM simplifies the original model drastically while retaining accuracy at an adequate level. Even though the simplest EWB model is a 2nd order linear system, the best ROM vary depending on EWB design parameters.

Corresponding Author:

Mohd Hanif Che Hasan
Department of Electrical Engineering Technology, Faculty of Electrical Technology and Engineering
Universiti Teknikal Malaysia Melaka
15300 Durian Tunggal, Melaka, Malaysia
Email: hanif.hasan@utem.edu.my

1. INTRODUCTION

The brake by wire (BBW) is a next-generation brake system that entirely replaces the traditional brake mechanism. The electro-mechanical brake (EMB) is the most accurate description of BBW because electronically powered actuators generate the braking force. The EMB has the following advantages: it is noiseless, has a faster response time, is easy to create a control system, and is more ecologically friendly [1]. Most EMBs have an electric motor, a reduction gear, a floating disc brake calliper, and a 24/42 V power supply [2], [3], and consume a lot of energy [4]. Since existing automobiles only use a 12 V power supply, the electronic wedge brake (EWB) technology has been a popular alternative because it can run at the same voltage as the power source and uses around one-tenth of the power [5]. The EWB is from the EMB category that, by employing the self-reinforcement principle, can reduce energy usage.

Two types of EWB designs are categorised based on their actuation angle. The first type is the tangential angle, where the actuation angle is parallel to the disk surface. For this configuration, the actuation angle is 0 degrees. Therefore, the clamping force acts perpendicularly to the actuation force produced by the motor. In comparison, the second type is the optimised angle, when the actuation angle is set at the same angle as the wedge angle [6]. As discussed in [7]–[11], different actuation angles are analysed using analytical and experimental approaches. It is found that the best driving angle is when it is set equivalent to the wedge angle.

The EWB system can be modelled using physical modelling or system identification (SI). The SI method has been used to develop dynamic models of EWB such as Box-Behnken [12]. The physical modelling was first used in [6], where a state-space representation of the EWB model was used to construct a braking force controller. The EWB model was mathematically derived using ordinary differential equations (ODE) and was developed in three separate sub-assembly parts: the DC motor, lead screw, and EWB brake heart. As the investigation progresses, subsequent numbers of mathematical modelling of the EWB system have been developed [13]–[20]. In the EWB model, five states are identified: motor current, motor angular velocity, angular motor position, wedge speed, and wedge position. Three of these state vectors are derived from the motors and lead screw dynamics, while the other two are from the wedge model.

Furthermore, Hwang and Choi [21] describes the EWB model for tangential actuation type from an electric motor to a wedge mechanism in detail, with all differential equations for all components combined. However, the derived model was intended for basic EWB, which uses an actuation angle parallel to the disk surface (tangential type). Although the second-order system was widely used to describe wedge mechanism dynamics, there was also an 8th order system introduced to produce a model with at least 10% higher accuracy than others [22]. For this consideration, the entire EWB model mathematical description has up to the 13th order system after combining an electric motor (3rd order) and a roller screw (2nd order) dynamic. However, researchers did not use this model because of its enormous size and many parameters.

Due to the different types of actuation designs will have different model structures, the first flexible version of the EWB model is introduced, which can be used for two famous EWB designs based on tangential and optimised actuation angles [23]. The new generalised model is more compact and simpler than the various versions of EWB while retaining model accuracy. Despite the 5th order linear model being capable of describing the EWB system dynamic well, some nonlinearity is neglected in this model, such as gear backlashes, coulomb frictions, and disk gap clearance inherited from conventional EMB [24].

Model-based approaches, which are prevalent in modern control strategies, benefit significantly from representation in state space. Modern control strategies applied on EWB so far such as proportional-integral-derivative (PID) [2], [6], linear quadratic regulator (LQR) [25], Youla parameterisation [26], sliding mode control (SMC) [17], [21], and active disturbance rejection control (ADRC) [17] is highly dependent on a model that represents the actual model. The model order reduction (MOR) simplifies controller design for complex models. It falls into two categories: conceptual and mathematical/numerical/data-driven [27]. Model reduction of linear-nonparametric dynamical systems has reached a considerable level of maturity. However, parametric model reduction has emerged more recently as an important and vibrant research area [28]. Even though research in parametric model reduction now mainly concentrates on nonlinear, parameterised, and coupled problems, linear problems are still some unexplored challenges, especially in certain applications.

Reducing the complexity of the 5 separate states involved in designing a controller for EWB is difficult due to limited sensor access. However, neglecting certain factors such as motor inductance, lead screw axial damping, and wedge mass can simplify the 5th order linear EWB model to a 2nd order linear system [21]. Nonetheless, no further research is done to see what happens if not all these variables are considered. Based on these three factors, we performed 2 cases based on our EWB parameters and realised that the number of factors that can be ignored depends on EWB design parameters [29]. Motivated by this result, we have expanded our study to several cases, as in this article and provided detailed derivation and assumptions. We proposed 6 cases with different EWB simplified models. Based on our EWB design, further analysis is made to evaluate each model accuracy, with the flexible, 5th order linear model being used as a benchmark. All the symbols and parameters used in this paper are based on previous work reported in [23].

There are four sections in this article. The first segment focuses on the EWB modelling review of other relevant work. The equations involved in complete parametric modelling of the EWB are then listed, followed by the 6 cases based on different scenarios. The simplified model for each case is proposed, and the output response of the model is simulated and observed based on step response (time-domain) and bode plot (frequency-domain) form. Besides, the root means square error (RMSE) value is used to find the best-simplified model before ending with the conclusion in the last section.

2. METHOD

2.1. Original model

As shown in Figure 1, the brake actuator consisted of the DC motor and the roller screw. The DC motor actuator was used in this system to move the input torque and force the centre brake through a roller screw, which transforms the angular motion of the DC motor into the axial motion of the coil in the centre of the brake. On the other hand, the heart of the brake, consisting of a wedge mechanism, a calliper, and a brake pad, may have diagonal motions, providing a clamping force to the brake disk.
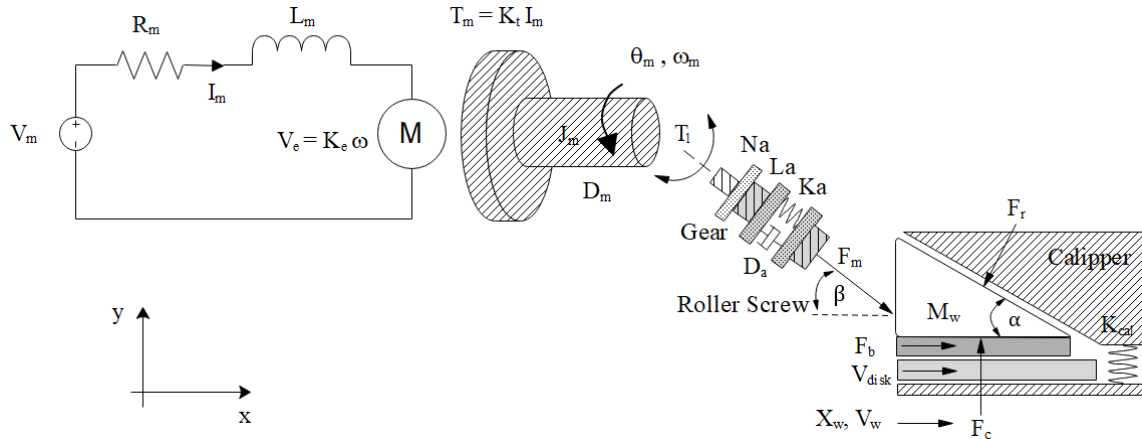
Figure 1. EWB schematic diagram

There is a total of 7 equations that represent the dynamic of the EWB system. Several terms are introduced to facilitate the derivative process as follows:

$$a_1 = K_{cal} \tan \alpha \, (\tan \alpha - \mu)$$

$$a_2 = M_w (\tan^2 \alpha + 1)$$

$$a_3 = \frac{L_a N_a}{2\pi}$$

$$a_4 = \cos \beta$$

Where

$$\beta = \begin{cases} 0 & \text{, for Tangential Actuation EWB} \\ \alpha & \text{, for Optimised Actuation EWB} \end{cases}$$

The complete model of EWB consists of a few physical parameters. The six parameters of DC motor are resistance (R_m), inductance (L_m), electromotive force constant (K_e), torque constant (K_t), inertia (J_m), and viscous friction constant (D_m). The lead screw consists of 5 parameters which are reduction gear ratio (N_a), steadiness (K_a), viscous damping (D_a), pitch (L_a), and efficiency (η). The wedge mechanism and brake pad parameters are wedge mass (M_w), wedge angle (α), actuation angle (β), calliper stiffness (K_{cal}), and brake pad coefficient (μ). The DC motor electrical and mechanical dynamics describe by (1) where Im is a motor current, θ_m is a motor angle, and ω_m is an angular speed of a DC motor.

$$\dot{I_m} = -\frac{K_e}{L_m} \omega_m - \frac{R_m}{L_m} I_m + \frac{1}{L_m} V_m \tag{1}$$

$$\dot{\omega_m} = -\frac{D_m}{J_m} \omega_m + \frac{K_t}{J_m} I_m - \frac{1}{J_m} T_{screw} \tag{2}$$

For the lead screw dynamic that connects DC motor and wedge, the motor force (F_m) and screw torque (T_{screw}) can be defined as (3) and (4):

$$F_m = K_a \left(a_3 \theta_m - \frac{X_w}{a_4}\right) + D_a \left(a_3 \dot{\theta}_m - \frac{V_w}{a_4}\right) \tag{3}$$

$$T_{screw} = a_3 \frac{F_m}{\eta} \tag{4}$$

Where X_w is a displacement and V_w is a speed of a wedge. By substituting (3) into (4), the torque screw (T_{screw}) can be defined as (5):

$$T_{screw} = \frac{a_3}{\eta} \left[K_a \left(a_3 \theta_m - \frac{X_w}{a_4}\right) + D_a \left(a_3 \dot{\theta}_m - \frac{V_w}{a_4}\right)\right] \tag{5}$$

For wedge mechanism dynamic is described as (6):

$$\dot{V_w} = \left(-\frac{a_1}{a_2}\right) X_w + \left(\frac{1}{a_2 a_4}\right) F_m \tag{6}$$

Note that these six equations used are the simplified version when the angle of actuation (β) can be either 0 or equal to wedge angle (α) as in [23]. Finally, the clamping force (F_c) of the wedge depends on the wedge displacement (X_w) in the x-direction, calliper stiffness (K_{cal}), and wedge angle (α).

$$F_c = K_{cal} X_w \tan \alpha \tag{7}$$

2.2. Assumptions

The first assumption that can be made is the motor inductance factor. Motor inductance usually has a minimal value, making it challenge to be a dominant pole. When this factor is ignored, (1) can be rewritten as (8):

$$I_m = -\frac{K_e}{R_m} \omega_m + \frac{1}{R_m} V_m \tag{8}$$

By substituting (8) into (2), both of DC motor equations is combined and become a single description.

$$\dot{\omega_m} = -\left(\frac{D_m}{J_m} + \frac{K_t K_e}{J_m R_m}\right) \omega_m + \left(\frac{K_t}{J_m R_m}\right) V_m - \frac{1}{J_m} T_{screw} \tag{9}$$

Meanwhile, the second possible assumption is based on the axial damping factor. In most cases where the mechanical component is so stiff, the axial damping only has little effect on the system response. Therefore, the equation for the axial connection in (3) and (5) can be rewritten as (10) and (11):

$$F_m = (K_a a_3) \theta_m - \left(\frac{K_a}{a_4}\right) X_w \tag{10}$$

$$T_{screw} = \left(\frac{K_a a_3{}^2}{\eta}\right) \theta_m - \left(\frac{K_a a_3}{\eta a_4}\right) X_w \tag{11}$$

The third assumption, on the other hand, is based on the mass of the wedge. In a typical EWB mechanical system, the light mass wedge is usually coupled with a high degree of stiffness. Thus, resulting to a stiff mechanical part with very high bandwidth. So, the performance of the system response largely depends on the electrical actuation system. Accordingly, the dynamic of a wedge is ignored by setting the mass of the wedge to zero. So that (6) is transformed into:

$$F_m = (a_1 a_4) X_w \tag{12}$$

In this study, 6 cases were selected for further evaluation. These cases were derived based on assumptions and resulted in state-space representations. The first 3 cases are based on a single factor being ignored: motor induction, axial damping, or wedge mass. The fourth and fifth cases are combinations of two factors being neglected. The sixth case considers a combination of all factors being neglected.

2.3. Case 1–neglection of DC motor inductance
In (13) yields when (5) is substituted into (9). Meanwhile, substituting (3) into (6) yields (14):

$$\dot{\omega}_m = \left(\frac{K_a a_3}{\eta J_m a_4}\right) X_w + \left(\frac{D_a a_3}{\eta J_m a_4}\right) V_w - \left(\frac{K_a a_3^2}{\eta J_m}\right) \theta_m - \left(\frac{D_m}{J_m} + \frac{K_t K_e}{J_m R_m} + \frac{D_a a_3^2}{\eta J_m}\right) \omega_m + \left(\frac{K_t}{J_m R_m}\right) V_m \qquad (13)$$

$$\dot{V}_w = -\left(\frac{K_a + a_1 a_4^2}{a_4 a_2^2}\right) X_w - \left(\frac{D_a}{a_2 a_4^2}\right) V_w + \left(\frac{K_a a_3}{a_2 a_4}\right) \theta_m + \left(\frac{D_a a_3}{a_2 a_4}\right) \omega_m \qquad (14)$$

Using (7), (13), and (14) will reduce the order of state-space and hence, yields:

$$\begin{aligned}\dot{x} &= Ax + Bu \\ y &= Cx + Du\end{aligned} \qquad (15)$$

$$x = [X_w, V_w, \theta_m, \omega_m]^T$$
$$y = F_c$$

$$A = \begin{bmatrix} 0 & 1 & 0 & 0 \\ -\frac{K_a + a_1 a_4^2}{a_2 a_4^2} & -\frac{D_a}{a_2 a_4^2} & \frac{K_a a_3}{a_2 a_4} & \frac{D_a a_3}{a_2 a_4} \\ 0 & 0 & 0 & 1 \\ \frac{K_a a_3}{\eta J_m a_4} & \frac{D_a a_3}{\eta J_m a_4} & -\frac{K_a a_3^2}{\eta J_m} & -\frac{D_m}{J_m} - \frac{K_t K_e}{J_m R_m} - \frac{D_a a_3^2}{\eta J_m} \end{bmatrix}$$

$$B = \begin{bmatrix} 0 \\ 0 \\ 0 \\ \frac{K_t}{J_m R_m} \end{bmatrix}, \quad and \ C = \begin{bmatrix} K_{cal} \tan(\alpha) \\ 0 \\ 0 \\ 0 \end{bmatrix}^T$$

Therefore, system order reduces by 1 when neglecting motor inductance. The EWB model then becomes a fourth order system with four state vectors instead of the fifth order in its original model.

2.4. Case 2–neglection of axial damping

In the 2nd case, (16) yields by substituting (10) into (6). Furthermore, substituting (11) into (2) produces (17).

$$\dot{V}_w = -\left(\frac{K_a + a_1 a_4^2}{a_2 a_4^2}\right) X_w + \left(\frac{K_a a_3}{a_2 a_4}\right) \theta_m \qquad (16)$$

$$\dot{\omega}_m = \left(\frac{K_a a_3}{\eta J_m a_4}\right) X_w - \left(\frac{K_a a_3^2}{\eta J_m}\right) \theta_m - \left(\frac{D_m}{J_m}\right) \omega_m + \left(\frac{K_t}{J_m}\right) I_m \qquad (17)$$

Finally, by combining (1), (7), (16), and (17), the complete model of the EWB actuator without axial damping dynamic factor is obtained:

$$x = [X_w, V_w, \theta_m, \omega_m, I_m]^T \qquad (18)$$

$$A = \begin{bmatrix} 0 & 1 & 0 & 0 & 0 \\ -\frac{K_a + a_1 a_4^2}{a_2 a_4^2} & 0 & \frac{K_a a_3}{a_2 a_4} & 0 & 0 \\ 0 & 0 & 0 & 1 & 0 \\ \frac{K_a a_3}{\eta J_m a_4} & 0 & -\frac{K_a a_3^2}{\eta J_m} & -\frac{D_m}{J_m} & \frac{K_t}{J_m} \\ 0 & 0 & 0 & -\frac{K_e}{L_m} & -\frac{R_m}{L_m} \end{bmatrix}$$

$$B = \begin{bmatrix} 0 \\ 0 \\ 0 \\ 0 \\ \frac{1}{L_m} \end{bmatrix}, \quad and \ C = \begin{bmatrix} K_{cal} \tan(\alpha) \\ 0 \\ 0 \\ 0 \\ 0 \end{bmatrix}^T$$

In this case, even though the system is simplified, the system order remains like the original model.

2.5. Case 3–neglection of wedge mass

Negligence for case 3 is possible when the wedge mass is very light. From (12) is substituted into (4) and then substituted into the motor in (2) will yields (19). Meanwhile, (12) with (3) will produces (20).

$$\dot{\omega}_m = -\left(\frac{a_1 a_3 a_4}{\eta J_m}\right) X_w - \frac{D_m}{J_m}\omega_m + \frac{K_t}{J_m}I_m \tag{19}$$

$$\dot{X}_w = -\left(\frac{K_a + a_1 a_4^2}{D_a}\right) X_w + \left(\frac{K_a a_3 a_4}{D_a}\right)\theta_m + (a_3 a_4)\omega_m \tag{20}$$

By combining (1), (7), (19), and (20), the reduced order model (ROM) for case 3 is produced.

$$x = [X_w, \theta_m, \omega_m, I_m]^T \tag{21}$$

$$A = \begin{bmatrix} -\frac{K_a + a_1 a_4^2}{D_a} & \frac{K_a a_3 a_4}{D_a} & a_3 a_4 & 0 \\ 0 & 0 & 1 & 0 \\ -\frac{a_1 a_3 a_4}{\eta J_m} & 0 & -\frac{D_m}{J_m} & \frac{K_t}{J_m} \\ 0 & 0 & -\frac{K_e}{L_m} & -\frac{R_m}{L_m} \end{bmatrix}$$

$$B = \begin{bmatrix} 0 \\ 0 \\ 0 \\ \frac{1}{L_m} \end{bmatrix}, \quad and \quad C = \begin{bmatrix} K_{cal}\tan(\alpha) \\ 0 \\ 0 \\ 0 \end{bmatrix}^T$$

Therefore, system order reduces by one when considering wedge mass is very light. The EWB model becomes a fourth-order system with four state vectors instead of the fifth order in its original model.

2.6. Case 4–neglection of motor inductance and axial damping

In case 4, (11) is substituted into a simplified equation for neglecting motor inductance case as in (9), which then produces (22):

$$\dot{\omega}_m = \left(\frac{K_a a_3}{J_m \eta a_4}\right) X_w - \left(\frac{K_a a_3^2}{J_m \eta}\right)\theta_m - \left(\frac{D_m}{J_m} + \frac{K_t K_e}{J_m R_m}\right)\omega_m + \left(\frac{K_t}{J_m R_m}\right)V_m \tag{22}$$

Using (7), (16), and (22), the ROM size of the state-space yields (23):

$$x = [X_w, V_w, \theta_m, \omega_m]^T \tag{23}$$

$$A = \begin{bmatrix} 0 & 1 & 0 & 0 \\ -\frac{K_a + a_1 a_4^2}{a_2 a_4^2} & 0 & \frac{K_a a_3}{a_2 a_4} & 0 \\ 0 & 0 & 0 & 1 \\ \frac{K_a a_3}{\eta J_m a_4} & 0 & -\frac{K_a a_3^2}{\eta J_m} & -\frac{D_m}{J_m} - \frac{K_t K_e}{J_m R_m} \end{bmatrix}$$

$$B = \begin{bmatrix} 0 \\ 0 \\ 0 \\ \frac{K_t}{J_m R_m} \end{bmatrix}, \quad and \quad C = \begin{bmatrix} K_{cal}\tan(\propto) \\ 0 \\ 0 \\ 0 \end{bmatrix}^T$$

2.7. Case 5–neglection of axial damping and wedge mass

For the 5th case where axial damping and wedge mass are ignored. In (10) with (12) produces (24). Meanwhile, (25) yields by substituting (22) into (17).

$$X_w = \left[\frac{K_a a_3 a_4}{K_a + a_1 a_4^2}\right]\theta_m \tag{24}$$

$$\dot{\omega}_m = \left(\frac{K_a^2 a_3^2}{\eta J_m(K_a + a_1 a_4^2)} - \frac{K_a a_3^2}{\eta J_m}\right)\theta_m - \left(\frac{D_m}{J_m}\right)\omega_m + \left(\frac{K_t}{J_m}\right)I_m \tag{25}$$

Substituting (24) into (7) generates:

$$F_c = K_{cal}\, tan\, \alpha \left(\frac{K_a a_3 a_4}{K_a + a_1 a_4^2}\right)\theta_m \tag{26}$$

Finally, by combining (1), (25) and (26), the complete model of the EWB actuator when axial damping and wedge mass are neglected is obtained.

$$x = [\theta_m, \omega_m, I_m]^T \tag{27}$$

$$A = \begin{bmatrix} 0 & 1 & 0 \\ \frac{K_a^2 a_3^2}{\eta J_m(K_a + a_1 a_4^2)} - \frac{K_a a_3^2}{\eta J_m} & -\frac{D_m}{J_m} & \frac{K_t}{J_m} \\ 0 & -\frac{K_e}{L_m} & -\frac{R_m}{L_m} \end{bmatrix}$$

$$B = \begin{bmatrix} 0 \\ 0 \\ \frac{1}{L_m} \end{bmatrix}, \quad and \quad C = \begin{bmatrix} \frac{K_{cal}\, tan(\infty)K_a a_3 a_4}{K_a + a_1 a_4^2} \\ 0 \\ 0 \end{bmatrix}^T$$

Therefore, in this case, the system order reduces by 2. The simplified model of EWB becomes a third-order linear system. In this case, an estimated transient behaviour purely comes from motor behaviour.

2.8. Case 6–neglection of all 3 factors

The maximum reduction of the model can be made by assuming that all of the three aforementioned factors can be ignored. Substituting (24) into (22) produces the single as (28):

$$\dot{\omega}_m = -\left[\frac{K_a a_3^2}{\eta J_m}\left(\frac{a_1 a_4^2}{K_a + a_1 a_4^2}\right)\right]\theta_m - \left(\frac{D_m}{J_m} + \frac{K_t K_e}{J_m R_m}\right)\omega_m + \left(\frac{K_t}{J_m R_m}\right)V_m \tag{28}$$

Using (26) and (28), the EWB ROM in the state-space is obtained.

$$x = [\theta_m, \omega_m]^T \tag{29}$$

$$A = \begin{bmatrix} 0 & 1 \\ -\frac{K_a a_3^2}{\eta J_m}\left(\frac{a_1 a_4^2}{K_a + a_1 a_4^2}\right) & -\frac{D_m}{J_m} - \frac{K_t K_e}{J_m R_m} \end{bmatrix}$$

$$B = \begin{bmatrix} 0 \\ \frac{K_t}{J_m R_m} \end{bmatrix}, \quad and \quad C = \begin{bmatrix} \frac{K_{cal}\, tan(\infty)K_a a_3 a_4}{K_a + a_1 a_4^2} \\ 0 \end{bmatrix}^T$$

Thus, the system can be represented only with a motor angle (θ_m) and motor angular speed (ω_m) in the simplest model. The system order is reduced from five to two.

3. RESULTS AND DISCUSSION

Based on derived state-space via MOR discussed before, it concludes that the size and complexity of an EWB model are possibly be reduced by using 3 possible assumptions. The original model which is a 5th order system can be reduced as low as a 2nd order system and summarised in Table 1. The best ROM is chosen for its accuracy and simplicity. Assumptions for controller design are determined. Frequency and time-based analyses were performed using a bode plot and step response. 5th order EWB model was used to evaluate the accuracy of simplified models.

Frequency-based analysis of six ROMs is plotted in two bode plot forms as in Figures 2 and 3. From both figures, only several cases are considered acceptable. Only cases 2, 3, and 5 were permitted while

showing results close to the benchmark model. The case 2 bode plot follows the benchmark model closely when compared to others for both the magnitude and phase values. Cases 3 and 5 also follow the benchmark model closely at low-level frequency. However, both models start showing different behaviours at a high frequency that starts from 30 k rad/s and above.

Table 1. The EWB ROM in state space summary

Case no.	Neglecting factor	Independence states	Clamping force (F_c)
1	Motor inductance (L_m)	$X_w, V_w, \theta_m, \omega_m$	Obtain from X_w
2	Axial damping (D_a)	$X_w, V_w, \theta_m, \omega_m, I_m$	Obtain from X_w
3	Wedge mass (M_w)	$X_w, \theta_m, \omega_m, I_m$	Obtain from X_w
4	Motor inductance (L_m) and axial damping (D_a)	$X_w, V_w, \theta_m, \omega_m$	Obtain from X_w
5	Axial damping (D_a) and wedge mass (M_w)	θ_m, ω_m, I_m	Estimate from θ_m
6	Motor inductance (L_m), axial damping (D_a), and wedge mass (M_w)	θ_m, ω_m	Estimate from θ_m
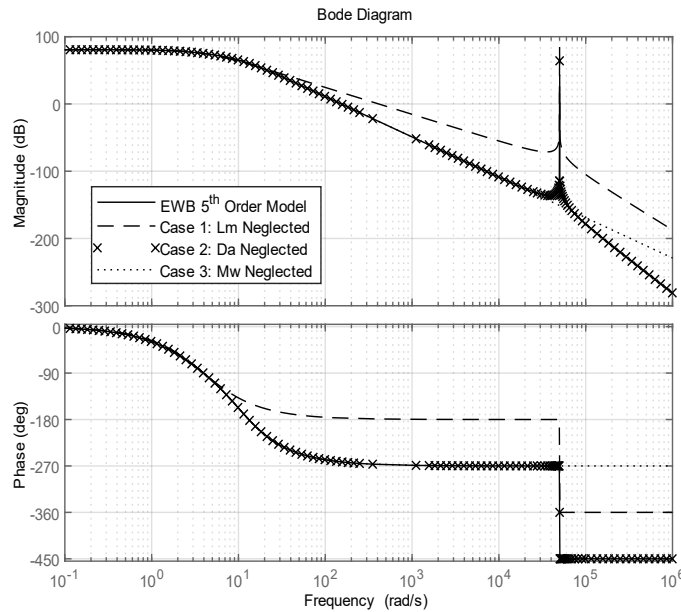
Figure 2. The bode plot of the EWB original model versus first 3 cases of ROMs
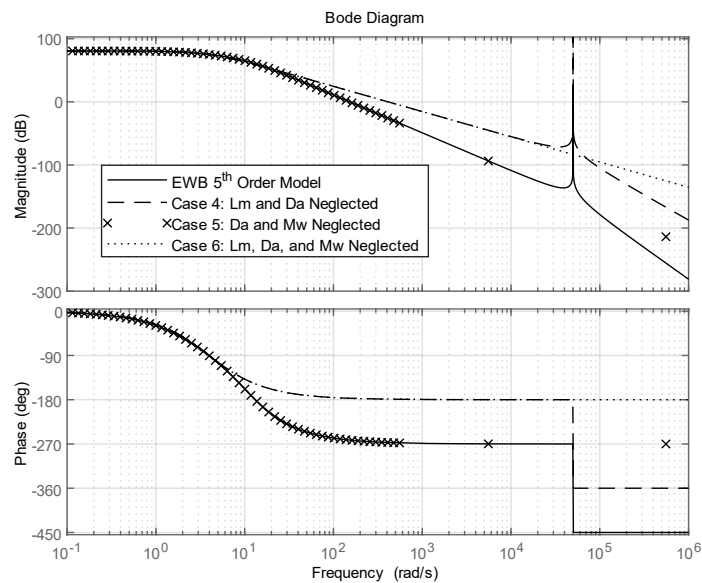
Figure 3. The bode plot of the EWB original model versus last 3 cases of ROMs

The accuracy of the proposed ROMs was further analysed using the time domain. For a simplified comparison, two groups of proposed models were made. Cases 1, 4, and 6 ROMs that showed different behaviour compared to the benchmark model are placed in the A group. Meanwhile, group B consists of the ROMs (2, 3, and 5) that offers a similar response to the benchmark. The clamping force is the output for the EWB model. The model output for each proposed model is plotted based on their group, according to the frequency-based accuracy result mentioned earlier. The clamping force response of each approximate model are as plotted in Figures 4(a) and (b).

The step response shown in Figure 4(a) reveals that cases 1, 4, and 6 (group A) have a relatively large error. Two parts of the responses show errors from 0.1 to 0.3 seconds and 0.75 to 1.75 seconds, as highlighted in the graph. Meanwhile, the other group (group B) show very high accuracy responses which are close to the benchmark model, as in Figure 4(b). The model responses in the graph at 0.95 to 1.05 seconds showed no error spotted even though the graph was enlarged.
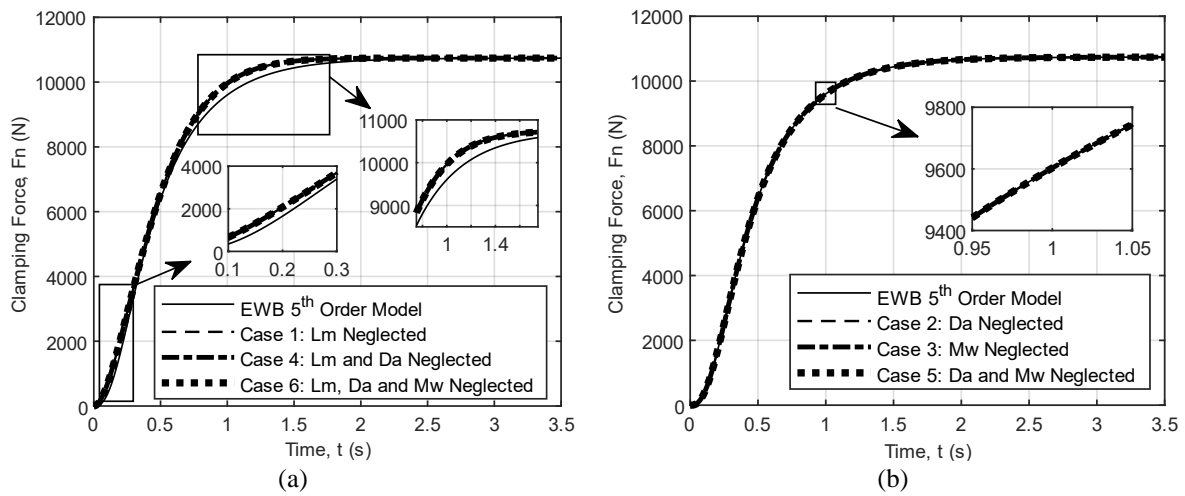
Figure 4. ROM clamping force step response for; (a) group A and (b) group B

Based on the step response analysis, it is difficult to evaluate the accuracy of each model since the error is minimal and cannot be observed by normal observation. Therefore, the responses of both group models were investigated further by plotting the clamping force error, as in Figure 5. As displayed in Figure 5(a), the error for cases 1, 4, and 6 (group A) show the same magnitude and pattern. Figure 5(b) on the other hand, demonstrates the group B model deficient error, where it was found that the case 2 model accuracy is the best, followed by case 5 and case 3 models. The graph show that the error occurs only during the transient state and goes down to zero as time goes to infinity.
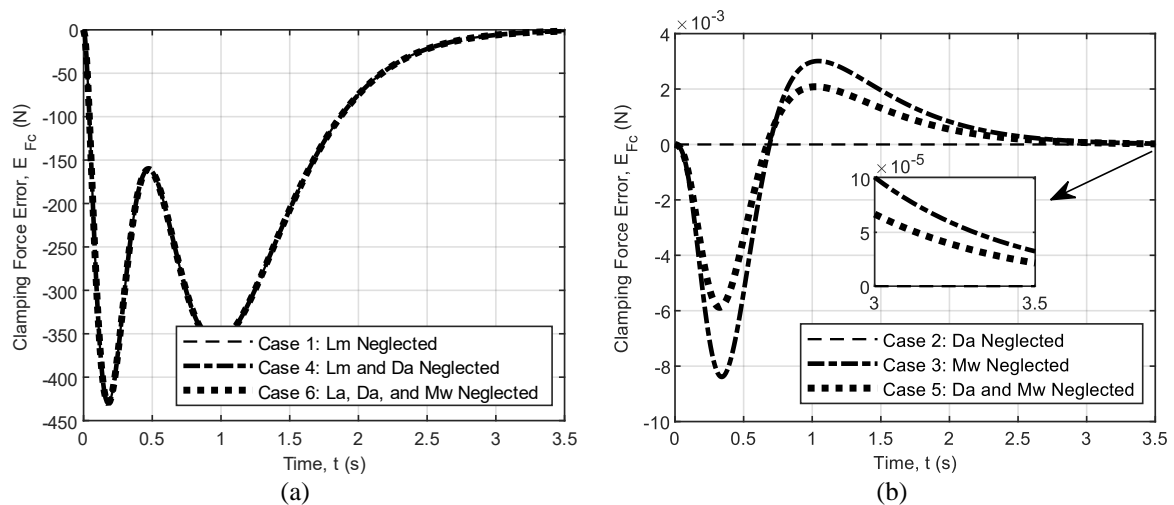

Figure 5. ROM clamping force error for; (a) group A and (b) group B

In addition, the commonly used RMSE value was used to calculate the average error for the entire time range of the model response errors. The RMSE value and percentage for each approximated model are summarised in Table 2. The RMSE for case 2 was found to be the least with only 5.23e-12%, followed by case 5 and case 3 with 1.94e-5% and 2.80e-5%, respectively. Even though have a simpler system with almost zero error, the model reduction size produced in case 2 does not change. The best model reduction for case 5 gives the simplest model with an acceptable error value. It is clearly shown that based on our design, only 3 states are dominant which are motor position (θ_m), motor speed (ω_m), and motor current (I_m).

Table 2. The RMSE of clamping force for EWB reduce order ROMs

Proposed model case number	RMSE value (N)	RMSE percentage (%)
1	198.92	2.08
2	5.00e-10	5.23e-12
3	2.70e-3	2.80e-5
4	198.92	2.08
5	1.90e-3	1.94e-5
6	198.92	2.08

4.   CONCLUSION

The EWB parametric MOR is possible and can be made based on 3 main factors. The motor inductance, lead screw axial damping, and wedge mass are the factors that may have little influence on the overall system. The EWB widely used 5th full order model can be reduced up to 2nd order system, depending on the design of the EWB itself which has its parameters. Time and frequency domain response analysis is compulsory to determine which factor can be neglected and consequently choose the suitable ROM that can be applied. The RMSE can be used to select the best ROM. Even though the simplest EWB model is a 2nd order linear system, the best simplifications model may vary depending on EWB design parameters.

REFERENCES

[1]   W. A. S. P. Abeysiriwardhana and A. M. H. S. Abeykoon, "Brake by wire control with pedal feedback and brake boost," *Bulletin of Electrical Engineering and Informatics*, vol. 10, no. 6, pp. 3042–3051, Dec. 2021, doi: 10.11591/eei.v10i6.3186.

[2]   H. Hartmann, M. Schautt, A. Pascucci, and B. Gombert, "eBrake® - The Mechatronic Wedge Brake," in *SAE Technical Paper*, Oct. 2002, p. 8, doi: 10.4271/2002-01-2582.

[3]   C. Li *et al.*, "A Review of Electro-Mechanical Brake (EMB) System: Structure, Control and Application," *Sustainability*, vol. 15, no. 5, p. 4514, Mar. 2023, doi: 10.3390/su15054514.

[4]   B. D. M. Gombert, M. Schautt, and R. P. Roberts, "The Development of Alternative Brake Systems," in *Encyclopedia of Automotive Engineering*, Wiley, 2014, pp. 1–11, doi: 10.1002/9781118354179.auto025.

[5]   K. Han, K. Huh, W. Hwang, M. Kim, and D. Kim, "EWB Control Based on the Estimated Clamping Force," in *SAE Technical Paper*, Sep. 2012, p. 11, doi: 10.4271/2012-01-1797.

[6]   J. Fox, R. Roberts, C. Baier-Welt, L. M. Ho, L. Lacraru, and B. Gombert, "Modeling and Control of a Single Motor Electronic Wedge Brake," in *SAE Technical Paper*, Apr. 2007, pp. 321–331, doi: 10.4271/2007-01-0866.

[7]   D.-H. Shin *et al.*, "Analytic approaches for keeping high braking efficiency and clamping efficiency of electro wedge brakes," *International Journal of Precision Engineering and Manufacturing*, vol. 16, no. 7, pp. 1609–1615, Jun. 2015, doi: 10.1007/s12541-015-0211-1.

[8]   J. Wang, Y. Zhang, D. Song, and Q. Wang, "Parameters design and braking efficiency analysis of a hydraulic self-energizing wedge disc brake," *International Journal of Precision Engineering and Manufacturing*, vol. 18, no. 10, pp. 1409–1418, Oct. 2017, doi: 10.1007/s12541-017-0168-3.

[9]   K. R. M. Mahmoud, M. M. Makrahy, K. A. A. El Gwwad, N. M. Ghazaly, and A. M. A. El Tawwab, "Effect of wedge inclination angle on self-amplification action of a new adaptive wedge disc brake," *International Journal of Vehicle Performance*, vol. 2, no. 2, p. 166, 2016, doi: 10.1504/IJVP.2016.075354.

[10]   H. M. Abdel-Rahman, A. O. Moaaz, N. M. Ghazaly, and A. M. A. El Tawwab, "Investigation of a new wedge disc brake mechanism," *International Journal of Mechanical and Production Engineering Research and Development*, vol. 9, no. 6, pp. 585–594, 2019.

[11]   M. M. Makrahy, N. M. Ghazaly, K. A. A. El-Gwwad, K. R. Mahmoud, and A. M. Abd-El-Tawwab, "A Preliminary Experimental Investigation of a New Wedge Disc Brake," *International Journal of Engineering Research and Applications*, vol. 3, no. 6, pp. 735–744, 2013.

[12]   N. M. Ghazaly, M. M. Makrahy, K. A. A. E. Gwwad, K. R. Mahmoud, and A. M. A. E. Tawwab, "Experimental Evaluation of an Empirical Model for Wedge Disc Brake using Box-Behnken Design," *International Journal of Vehicle Structures and Systems*, vol. 6, no. 3, pp. 58–63, Aug. 2014, doi: 10.4273/ijvss.6.3.03.

[13] C. Jo, S. Hwang, and H. Kim, "Clamping-Force Control for Electromechanical Brake," *IEEE Transactions on Vehicular Technology*, vol. 59, no. 7, pp. 3205–3212, Sep. 2010, doi: 10.1109/TVT.2010.2043696.

[14] M. A. A. Emam, A. S. Emam, S. M. El-Demerdash, S. M. Shaban, and M. A. Mahmoud, "Performance of Automotive Self Reinforcement Brake System," *Journal of Mechanical Engineering*, vol. 1, no. 1, pp. 4–10, 2012.

[15] A. Ghajari and R. Kazemi, "A New Approach to the Electronic Wedge Brake," in *SAE Technical Paper*, Sep. 2012, p. 11, doi: 10.4271/2012-01-1801.

[16] K. Han, M. Kim, and K. Huh, "Modeling and control of an electronic wedge brake," *Proceedings of the Institution of Mechanical Engineers, Part C: Journal of Mechanical Engineering Science*, vol. 226, no. 10, pp. 2440–2455, Oct. 2012, doi: 10.1177/0954406211435584.

[17] F. Xu and C. Cho, "A Novel Electronic Wedge Brake Based on Active Disturbance Rejection Control," *Energies*, vol. 15, no. 14, p. 5096, Jul. 2022, doi: 10.3390/en15145096.

[18] M. S. Jneid, M. Zöldy, and P. Harth, "Sensorless optimal control of electronic wedge brake based on dynamic model and Kalman filter state multiple-estimation," *Proceedings of the Institution of Mechanical Engineers, Part D: Journal of Automobile Engineering*, Apr. 2023, doi: 10.1177/09544070231168168.

[19] M. Yao, J. Miao, S. Cao, S. Chen, and H. Chai, "The Structure Design and Optimization of Electromagnetic-Mechanical Wedge Brake System," *IEEE Access*, vol. 8, pp. 3996–4004, 2020, doi: 10.1109/ACCESS.2019.2962559.

[20] Q. Liu, L. Chen, and J. Chen, "Analytical Study on Dynamics of Wedge Braking Systems with Time Delay," *INTER-NOISE 2019 MADRID - 48th International Congress and Exhibition on Noise Control Engineering*, pp. 5627–5638, 2019.

[21] Y. Hwang and S. B. Choi, "Robust control of electronic wedge brake with adaptive pad friction estimation," *International Journal of Vehicle Design*, vol. 62, no. 2/3/4, p. 165, 2013, doi: 10.1504/IJVD.2013.052709.

[22] L. Balogh, T. Stréli, H. Németh, and L. Palkovics, "Modelling and simulating of self-energizing brake system," *Vehicle System Dynamics*, vol. 44, no. sup1, pp. 368–377, Jan. 2006, doi: 10.1080/00423110600872267.

[23] M. H. C. Hasan, M. K. Hassan, F. Ahmad, and M. H. Marhaban, "A dynamic model of electronic wedge brake: experimental, control and optimization," *Indonesian Journal of Electrical Engineering and Computer Science*, vol. 23, no. 2, pp. 740–751, Aug. 2021, doi: 10.11591/ijeecs.v23.i2.pp740-751.

[24] J. Kwak, B. Yao, and A. Bajaj, "Analytical Model Development and Model Reduction for Electromechanical Brake System," in *Dynamic Systems and Control, Parts A and B*, ASMEDC, Jan. 2004, pp. 297–306, doi: 10.1115/IMECE2004-61955.

[25] M. S. Jneid and A. Joukhadar, "LQR-Based Control of a Single Motor Electronic Wedge Brake EWB for Automotive Brake-By-Wire System," *Soft Computing and Electrical Engineering*, vol. 1, no. 1, pp. 12–35, 2019.

[26] E. Arasteh and F. Assadian, "A Comparative Analysis of Brake-by-Wire Smart Actuators Using Optimization Strategies," *Energies*, vol. 15, no. 2, p. 634, Jan. 2022, doi: 10.3390/en15020634.

[27] M. S. Mannan, W. J. Rogers, M. Gentile, and T. M. O'Connor, "Multiscale Modeling for Process Safety Applications," *Elsevier*, vol. 82, no. 3, 2016, doi: 10.1016/C2011-0-07976-0.

[28] P. Benner, S. Gugercin, and K. Willcox, "A Survey of Projection-Based Model Reduction Methods for Parametric Dynamical Systems," *SIAM Review*, vol. 57, no. 4, pp. 483–531, Jan. 2015, doi: 10.1137/130932715.

[29] M. H. C. Hasan, M. K. Hassan, F. Ahmad, and M. H. Marhaban, "Electronic wedge brake model approximation analysis," in *Proceedings of Mechanical Engineering Research Day 2020*, 2020, pp. 26–27.

BIOGRAPHIES OF AUTHORS

Mohd Hanif Che Hasan (corresponding author) received the B.Eng. degree in electrical engineering (mechatronic) from the Universiti Teknologi Malaysia (UTM), Skudai, Johor, Malaysia in 2003, and the M.Eng. degree in electrical-mechatronics and automatic control from the same university in 2013, and the Ph.D. degree in control system engineering from Universiti Putra Malaysia (UPM), Serdang, Selangor, Malaysia, in 2023. From 2003 to 2007, he was an engineer with the Mitsubishi Electric (M) Sdn. Bhd. Since 2007, he joins Universiti Teknikal Malaysia Melaka (UTeM), Malaysia as academic staff. His current research interests include applied control systems, image processing, SCADA, computer-based system, microcontroller, and PLC based applications. He can be contacted at email: hanif.hasan@utem.edu.my.

Mohd Khair Hassan received the B.Eng. degree in electrical and electronic engineering from the University of Portsmouth, U.K., in 1998, the M.Eng. degree in electrical engineering from Universiti Teknologi Malaysia (UTM), Skudai, Johor, Malaysia, in 2001, and the Ph.D. degree in automotive from Universiti Putra Malaysia (UPM), Serdang, Selangor, Malaysia, in 2011. He is currently an Associate Professor with the Department of Electrical and Electronic Engineering, UPM. His area of interest includes a control system, automotive control, electric vehicle, and AI applications. Currently, his focuses are on x-by-wire technology and optimal strategy for energy consumption in an electric vehicle. He is a Professional Engineer registered under the Board of Engineers Malaysia, a Corporate Member of the Institution of Engineers Malaysia, and a member of the Society of Automotive Engineers. He can be contacted at email: khair@upm.edu.my.

Fauzi Ahmad received the B.Eng. degree in mechanical engineering from Universiti Teknikal Malaysia Melaka, Malaysia (UTeM), in 2007, the M.Sc. degree in mechanical engineering (automotive) from same university in 2010, and the Ph.D. degree in automotive from Universiti Teknologi Malaysia (UTM)-MJIT, Semarak, Kuala Lumpur, Malaysia, in 2017. He is currently a Senior Lecturer with the Faculty of Mechanical Engineering, UTeM. His research interests include tire modelling, vehicle ride and handling and pneumatic system modelling and control. He can be contacted at email: fauzi.ahmad@utem.edu.my.

Mohammad Hamiruce Marhaban received the B.Eng. in Electrical and Electronics Engineering from the University of Salford in 2003. He then obtained his doctorate, Ph.D. in Electrical and Electronics Engineering, from the University of Surrey in 2003. His outstanding achievements in research, publications, supervision and consultancy led to his appointment as a Professor of UPM in 2015. Currently, he is the Director of the Research Management Centre of UPM. His research interests include artificial intelligence, computer vision, and robotics. He can be contacted at email: mhm@upm.edu.my.

Sharil Izwan Haris received the B.Eng. degree in mechanical engineering from Universiti Teknologi Malaysia (UTM), Skudai, Johor, Malaysia in 2003, and the M.Sc. degree in mechanical engineering from Universiti Teknikal Malaysia Melaka, Malaysia (UTeM), in 2016. He is currently pursuing the Ph.D. degree in automotive engineering at Universiti Teknikal Malaysia Melaka, Malaysia (UTeM), Melaka, Malaysia. He can be contacted at email: izwan.haris@mara.gov.my.

Ehsan Arasteh received a bachelor's degree in aerospace engineering and physics from Sharif University, Tehran, Iran, in 2015, and an M.Sc. degree in mechanical engineering from the University of California, Davis, United States. He is currently a Ph.D. candidate at the University of California, Davis. His research interests include vehicle dynamics, control theory, and autonomous vehicles. He can be contacted at email: earasteh@ucdavis.edu.